

## §11. Improvement of the Energy Resolved Soft X-ray Imaging System in LHD

Suzuki, C., Ida, K., Kobuchi, T. (Tohoku Univ.),  
Yoshinuma, M.

Soft X-ray CCD (Charge Coupled Device) cameras have recently been applied to imaging diagnostics of helical plasmas.<sup>1)</sup> If the energy resolved imaging is achieved, it can possibly be applied to the detection of the difference in two dimensional soft X-ray profile caused by local non-Maxwellian component of electron energy distribution function. For this end, we have already developed and demonstrated a diagnostic system for the energy resolved soft X-ray imaging by changing the filter thickness sequentially during a long pulse ICRH discharge of LHD. A tangential image for a specific photon energy range can be obtained by taking difference between two signals measured with different filters. In this fiscal year, the dependence of the measured signal intensity on the energy range was compared with the calculated one for continuum radiation for the initial analysis. In addition, we have replaced a supersonic motor driver and modified the timing system for better time resolution.

A schematic diagram of the present diagnostic system is shown in Fig. 1. The heart of the system is a soft X-ray CCD camera (Andor Technology, DO435-BV) equipped with a back illuminated CCD chip of frame transfer type. In the present study, we have employed 8 beryllium (Be) filters whose thicknesses range from 50 to 1650  $\mu\text{m}$ . The minimum time to complete one-step rotation of the filter disk is now shorter than 2 seconds by replacing the supersonic motor driver. Therefore the minimum acquisition cycle time equals the readout time of the CCD plus 2 seconds. The triggers for clockwise and counter-clockwise rotations of the filter disk are fed into a newly prepared personal computer, where commands are sent to the motor driver by a software via RS-232C interface.

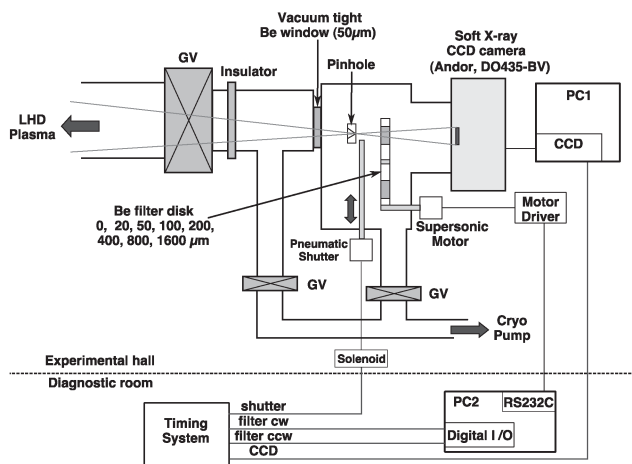


Fig. 1: Schematic diagram of the experimental setup.

As an initial analysis, it is possible to estimate roughly line-averaged effective electron temperature by comparing the measured dependences of the line-integrated signal intensities on the energy range with the calculated ones for various electron temperatures, assuming continuum radiation and spatially uniform effective charge ( $Z_{\text{eff}}$ ).<sup>2)</sup> The measured and calculated intensities against the photon energy at the maximum sensitivity for each filter combination are summarized in Fig. 2 plotted by solid and broken lines, respectively, for a typical shot. The circle and square symbols denote the experimental data in the central zone of the image obtained by CW and CCW rotations of the filter disk, respectively. The calculated intensities for the electron temperatures of 0.5, 0.7 and 1.0 keV are plotted by broken lines with the error bars due to the assumed thickness tolerance ( $\pm 10\%$ ) for the case of 0.7 keV. Though the most similar calculated data to the experimental one is for 0.7 keV, all data are within the large error bars due to the uncertainty in the filter thickness. Therefore actual uncertainty of the filter thickness should be precisely measured. In addition, the  $K_{\alpha}$  line radiations from metallic impurities would influence the observed signal intensity especially in higher energy range. In order to discuss spatial profiles in more detail, routines for the inversion of radial profiles based on a three dimensional equilibrium code is presently under preparation for the new system.

1) Liang, Y. et al.: Plasma Phys. Control. Fusion **44** (2002) 1383.

2) Suzuki, C. et al.: 34th EPS Conference, Warsaw, ECA 2007, Vol. 31F, P-2.139.

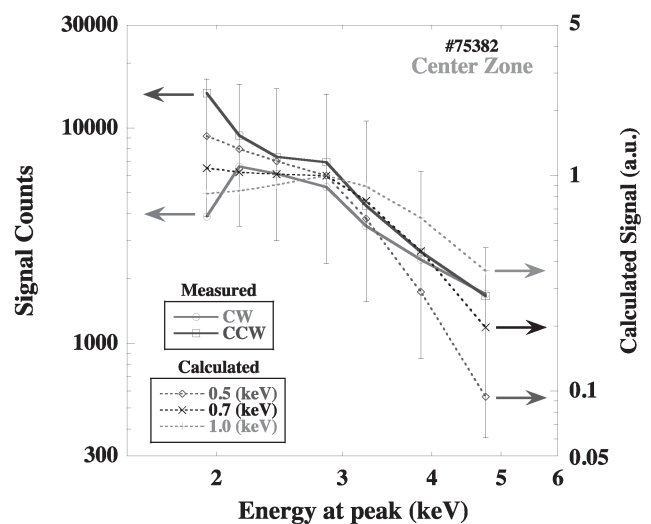


Fig. 2. The dependence of the signal intensity in the central zone on the photon energy range (solid lines). The calculated intensities for the electron temperatures of 0.5, 0.7 and 1.0 keV are also plotted by broken lines with the error bars due to the assumed thickness tolerance ( $\pm 10\%$ ) for 0.7 keV.